ADVANCED FUNCTIONAL MATERIALS

Phase-Separation-Induced Micropatterned Polymer Surfaces and Their Applications

By *Yong Wang*, *Zhimin Liu*,* *Buxing Han*,* *Zhenyu Sun*, *Jianling Zhang*, and *Donghai Sun*

We report a route to fabricate micropatterned polymer films with micro- or nanometer-scale surface concavities by spreading polymer solutions on a non-solvent surface. The route is simple, versatile, highly efficient, low-cost, and easily accessible. The concavity density of the patterned films is tuned from 10^6 to 10^9 features cm^{-2}, and the concavity size is controlled in the range from several micrometers to less than 100 nm, by changing the film-forming parameters including the polymer concentration, the temperature of the non-solvent and the interactions between polymer, solvent, and non-solvent. We further demonstrate that these concavity-patterned films have significantly enhanced hydrophobicity, owing to the existence of the surface concavities, and their hydrophobicity could be controlled by the concavity density. These films have been used as templates to successfully fabricate convex-patterned polymer films, inorganic TiO_2 microparticles, and NaCl nanocrystals. Their other potential applications are also discussed.

1. Introduction

Micropatterned polymer surfaces, on which there are many repeated, uniform and ordered two- or three-dimensional micro-architectures, possess many remarkable properties and functions as a result of their surface microstructures. These properties or functions are not intrinsic to the matrix materials for they as not present when the surface of the same polymer material remains unpatterned. For example, it was reported that, the shape of a water drop on the smooth surface of an isotactic polypropylene (i-PP) film had a contact angle of about 105°, which means the iPP film is only moderately hydrophobic. However, if it presents a gel-like porous surface, a superhydrophobic PP film with a contact angle of 160° could be obtained owing to the existence of many spongy aggregates on the surface of the PP film, which is a kind of micropattern, although not of a very uniform or ordered form.[1] Nowadays, thin films with a specially micropatterned surface have many other applications in modern science and technology, including in the microelectronics industry, in the field of biomedicine, etc.

Driven by increasingly enormous demands from industrial and scientific fields, a considerable variety of methodologies have been explored to pattern, on micro- or nanoscopic scales, the surface of materials. Recently, Xia and Whitesides published a review on the unconventional methods for fabricating and patterning nanostructures.[2] They categorized strategies for fabricating patterned nanostructures into five groups i) lithography with photons, particles, and scanning probes; ii) replication against masters (or molds) via physical contact; iii) -self-assembly; iv) templated deposition; and v) size reduction. Amongst these strategies, soft lithography[2,3] is one of the most intensively studied and documented methods. Soft lithography, which is a collective term including microcontact printing (μCP), replica molding (REM), micromolding in capillaries (MIMIC), microtransfer molding (μTM), and solvent-assisted micromolding (SAMIM), offers immediate advantages over photolithography and other conventional micropatterning techniques because of its simplicity, low cost, and accessibility.[4–10] For soft lithography, a pre-patterned elastomer, usually made of PDMS, is employed as the mold, stamp, or mask to generate or transfer the pattern.[2] That is to say, soft lithography is a template-assisted method. Before it can be used as a template to develop the pattern on a substrate, it is necessary to first pattern the mold itself, and for this one must resort to conventional photolighographic methods, thereby depleting the intrinsic advantages of soft lithography to some degree. As a template-free method, the self-assembly of phase-separated block copolymers can lead to stable, well-defined, micro-/nanoscale patterned structures, and has also been widely investigated.[11–13] However, the starting copolymers must be specially designed and synthesized, and the phase separation and self-assembly of the different segments in the copolymers occur only under strictly controlled thermodynamic conditions.

In our previous communication,[14] we presented a simple and novel route to micropatterned polymer surfaces through phase separation of the polymer solution spread on a non-solvent surface. We termed this method "SNS" (solvent–non-solvent). The starting materials that couldbe used in this method are many commercially available polymers, such as polystyrene (PS) and poly(methyl methacrylate) (PMMA), etc. The phase-separation process is induced by a non-solvent, and can be easily performed in a common chemistry laboratory. This method

[*] Dr. Z. Liu, Prof. B. Han, Y. Wang, Z. Sun,
Dr. J. Zhang, D. Sun
Center for Molecular Science
Joint Laboratory of Polymer Science and Materials
Institute of Chemistry, Chinese Academy of Sciences
Beijing 100080 (P.R. China)
E-mail: liuzm@iccas.ac.cn, hanbx@iccas.ac.cn

[**] This work is financially suppoted by National Natural Science Foundation of China (20073030, 20374057).

 DOI: 10.1002/adfm.200400201

is extremely simple and versatile. The surface patterns can be easily controlled and tuned by changing the conditions of phase separation of the polymer solution. In the present work, we study the effects of processing parameters on the morphologies of micropatterned polymer films, and discuss their mechanism of formation. We also investigate the wettability of the resultant micropatterned films, and employ the obtained micropatterned films as templates to fabricate micro- or nanomaterials, such as polymer films with convex-patterned surfaces, inorganic TiO_2 microparticles, and NaCl nanocrystals. The films prepared in this work also have potential applications as micro-optical components, cell-cultivating supports, micro-containers, and shortage media, and in controlled release, etc.

2. Results and Discussion

In this method, a drop (about 50 μL) of polymer solution, for example, PS in tetrahydrofuran (THF), was dripped on the surface of a non-solvent, typically, ethylene glycol (EG). The polymer solution droplet spread quickly on the non-solvent surface and solidified within several seconds, leading to an opaque or semi-transparent film. The resulted film was examined under a scanning electron microscope (SEM). Figure 1 gives SEM images of a PS film prepared by spreading a drop of 10 wt.-% PS/THF solution on an EG surface under ambient

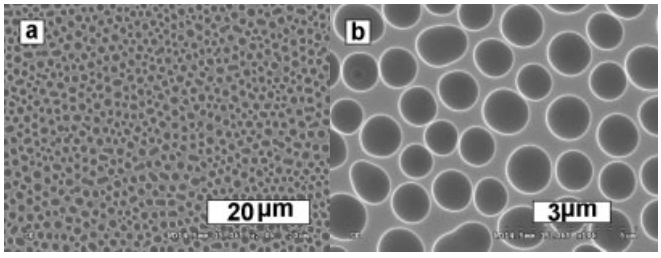

Figure 1. SEM images at different magnifications of the top surface of the patterned PS film prepared by spreading 50 μL of 10 wt.-% PS/THF solution on the EG surface at ambient conditions.

conditions. The film has a patterned top surface with many fairly uniform pores, the diameter of which is in the range 1.5–2.0 μm, and quite a high number density of up to 10^7 features cm^{-2}.

From an SEM image of a cross-section of the film reported in our previous work,[14] it can be observed that the film has a thickness of about 15 μm and contains many closed cellular pores, which have nearly the same diameter as the concavities on the top surface. However, on the bottom surface of the film (the side contacting the EG surface during the film-forming process), neither concavities nor pores could be observed, i.e., the bottom surface is rather smooth and non-patterned (see Fig. 4a).

2.1. Factors Influencing the Specific Film Pattern and Pattern Control

In the SNS method, the specific phase-separation procedure is dependent mainly on the system parameters, such as polymer concentration, temperature, and the interactions between solvent, polymer, and non-solvent, etc. In other words, the specific pattern of the obtained film is determined by these parameters. In the following we will discuss the effects of film-forming parameters on the size, shape, and density of the concavities on the patterned film.

2.1.1. Effect of Polymer Concentration

A change of polymer concentration in a solution will unavoidably influence the properties of the solution such as viscosity and mobility. We investigated the surface patterns of PS films prepared from solutions of different concentration[14] and Table 1 summaries data concerning the size, and density of the surface concavities of these films, as calculated from SEM images. The film that was prepared from a dilute polymer solution

Table 1. Size and density of the surface concavities of films prepared from solutions of different polymer concentration.

Polymer concentration [wt.-%]	Concavity size [μm]	Concavity density [features cm^{-2}]
5	2–6	1.0×10^6
10	1.5–2.0	2.8×10^7
15	0.4–0.6	2.1×10^8

(5 % PS in THF) was found to have patterns with disordered concavities ranged from 2 to 6 μm. However, the patterned concavities on the films prepared from 10 wt.-% and 15 wt.-% PS/THF solution are more uniform and their size distribution is much narrower. The poor-quality concave patterns of the film obtained from 5 wt.-% polymer solution may result from the lower viscosity and higher mobility of the more dilute solution, whose resistance to minor disturbance of environmental conditions during the film-forming process is poor. Therefore, the phase separation and also the concavity-forming procedure may be disturbed, giving rise to such a non-uniform concavity pattern. Obviously, we can easily draw the conclusion that the concavity size is reduced, while the density increases, as the polymer concentration is increased.

The concavities on the surface together with the cellular pores in the film may be a result of the nucleation and growth of the polymer-lean phase. In a concentrated solution, the nucleated polymer-lean phases have less solvent diffusing inward to keep the polymer-lean phases growing continuously, and the high viscosity in the concentrated solution limits their growth to some degree. The increase in the concavity density with polymer concentration may be explained by the idea that the concentrated polymer solution is more thermodynamically un-

ADVANCED FUNCTIONAL MATERIALS

stable and more readily to nucleate and form a polymer-lean phase, compared with the dilute polymer solution. It is also noticeable that the surface concavities on the film prepared from the 15 wt.-% PS/THF solution are not so circular in shape and are more irregularly shaped, while the concavities from the 10 and 5 wt.-% polymer solutions are spherical. This phenomenon may be attributed to the notion that in the concentrated solution, there are more polymer-lean phases formed and when they grow to a certain size, isotropically, in a radicalized mode, the neighboring nuclei, which are originally circular, approach each other and cluster together, thereby restricting their growth in some directions as a result of space limitations. Therefore, they lose their isotropic nature and form the irregularly shaped concavities.

2.1.2. Effects of the Non-Solvent Temperature

We also investigated the effects of the non-solvent temperature on the surface pattern by spreading PS/THF solution on the EG surface at different temperatures. Table 2 compares the concavity size and the density of the surface patterns fabricated at different non-solvent temperatures. Apparently, increasing non-solvent temperature leads to larger concavity size. This may be explained as follows: a rise in temperature reduces the viscosity of the system and increases the activity of the solvent and non-solvent. As a result, mass transfer through the polymer solution–non-solvent interface will proceed at a more rapid rate. In other words, the polymer-lean phases grow fast and result in larger pores or concavities in a unit time at higher temperature. From Table 2, we can see that the concavity density of the film prepared at the lowest non-solvent temperature (8 °C) is the largest, which can also be explained by the fact that the polymer solution at lower temperature is more thermodynamically unstable and phase separation can occur more readily than in the solution at a higher temperature. However, on the whole, unlike the polymer concentration, the non-solvent temperature does not influence the concavity density significantly in the temperature range investigated in our work. In addition, the concavities on the surface of the film prepared at 50 °C lose their original circular shape and become rough and irregular as a result of space limitations acting on neighboring concavities.

Table 2. Size and density of the surface concavities of films prepared at different non-solvent temperatures.

Non-solvent temperature [°C]	Concavity size [μm]	Concavity density [features cm^{-2}]
8	0.8–1.0	4.5×10^7
25	1.5–2.0	2.8×10^7
50	2.0–2.5	3.5×10^7

2.1.3. Effects of Solvent–Non-Solvent Interactions

The mutual affinity between solvent and non-solvent will significantly influence the phase-separation process, and further play an important role in the formation of the final film morphology.[15] First, we investigated the polymer–solvent–non-solvent systems by keeping the PS as the polymer component and EG as the non-solvent, while varying the solvent between cyclohexane, and chloroform, and THF. It was found that when THF was used as the solvent, the phase-separation process was complete within the shortest period (< 5 s), and resulted in an opaque, well-patterned film; while in the case of cyclohexane as the solvent, it took a much longer time (> 10 min) for the PS solution spread on the EG surface to be solidified, and the result was a nonporous dense film without any surface concavities. For the system with chloroform as the solvent, the phase behavior was similar to that of the PS–THF–EG system, but it took about 10 s to vitrify the PS solution, and, the result was a patterned film with fewer and much smaller concavities, compared with the PS–THF–EG system.

The difference of the phase-separation procedure and the final film morphology or pattern can be attributed to the difference of mutual affinity of the non-solvent towards the three solvents. EG is a strongly hydrogen-bonded polar solvent. However, cyclohexane (dielectric constant, $\varepsilon = 2.0$) is non-polar and has the worst affinity for polar EG. THF ($\varepsilon = 7.6$) is polar and can form hydrogen bonds with EG, and therefore shows the highest affinity for EG among the investigated solvents. The polarity of chloroform ($\varepsilon = 5.0$) is between that of cyclohexane and THF. In the PS–cyclohexane–EG system, due to the weakest solvent–non-solvent interaction, the exchange between the solvent and non-solvent across the polymer solution–non-solvent interface is very limited. The PS solution is solidified, mainly by the evaporation of the solvent to the air, which took a much longer time than a non-solvent-induced phase separation. In this case, the non-solvent served as an inert substrate, like a piece of glass, making the procedure similar to the process of air-casting a the polymer solution. For the cases of THF and chloroform, there is a certain affinity between the solvent and the non-solvent; thus, mass transfer and exchange between the solvent and non-solvent occur across the solution–non-solvent interface, and the liquid–liquid-demixing process vitrifies the polymer solution, resulting in patterned films. The solvent evaporation does not contribute significantly to the solidification of the polymer solution because this process is completed in a very short time (< 10 s). Furthermore, because EG has weaker affinity for chloroform than for THF, the exchange of chloroform for EG, and the nucleation and growth of the polymer-lean phase, proceed at a relatively slow rate. Therefore, the PS–chloroform–EG system needs a longer time to complete the phase-separation process, leading to a patterned film with fewer and smaller surface concavities, compared with the PS–THF–EG system.

Secondly, we investigated the polymer–solvent–non-solvent systems by keeping the PS as the polymer component and THF as the solvent, while changing the non-solvent in between water, EG, and glycerol (GC). Although all the three non-solvents have strong polarities, they behave very differently towards the PS/THF solution and result in patterned films with different types of order. Compared with the surface pattern from PS–THF–EG system, shown in Fig. 1, films produced from water and GC both feature lower concavity densities, and wide distributions of concavity density, especially for the PS–THF–water system. Of course, the lesser degree of order is related to the specific phase-separation process (although the solvent THF shows similar miscibility toward water, EG, and GC). In the PS–THF–water system, there is a violent solvent–non-solvent exchange across the PS-solution–non-solvent interface due to the relatively strong mutual affinity between THF and water, and, as a result, a pattern with wide size distribution is obtained. In the case of GC as the non-solvent, if we only take the solvent–non-solvent mutual affinity into consideration, there should also be a violent mass transfer across the interface, just like for the PS–THF–water system. However, due to larger GC molecule size, together with its larger density and viscosity, it is more difficult for GC to diffuse upward into the PS solution side of the interface through the pre-formed dense skin. Therefore, the mass transfer across the PS-solution/GC interface is almost one-way, dominated by the relatively slow diffusion of THF into the GC side through the dense skin. The vitrification of the polymer solution results from the leaching of the solvent by diffusion downward into the GC side. In this case, loss of solvent through the evaporation of the solvent into the air is more noticeable because of a slower and longer phase-separation process. Consequently, fewer concavities with small diameter are formed on the film surface. As for EG, it has a molecule size, density, and viscosity intermediate between water and GC, and therefore, a moderate mass transfer with the solvent THF through the interface. This results in a well-patterned surface with a relatively narrow distribution of concavity sizes.

From the above discussion, we know that the solvent–non-solvent interactions play an essential role in the phase-separation process and further significantly influence the final film pattern. In order to get a well-patterned film surface, it is key to select an appropriate solvent–non-solvent pair which possesses a proper interaction to ensure that the phase-separation process proceeds at a moderate rate, i.e., not too fast and not too slow. In other words, it shows the possibility to control and adjust the pattern mode on the film surface by changing the solvent–non-solvent pairs. For example, in this work we fabricated PS films with surface concavities of < 100 nm diameter and density up to $4.6 \times 10^9\,cm^{-2}$ by using a room-temperature ionic liquid (RTIL), 1-butyl-3-methylimidazolium hexafluorophosphate, [bmim]PF_6, as the non-solvent (Fig. 2), due to a proper mutual affinity between THF and [bmim]PF_6.

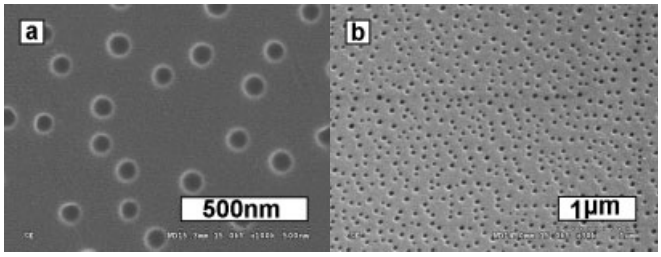

Figure 2. SEM images at different magnifications of the patterned surface from PS–THF–[bmim]PF_6 system.

In addition, we demonstrated that polymer–solvent–non-solvent systems using polymers other than PS can also be applied to fabricate patterned films. We also obtained patterned surfaces from the system of PMMA–THF–EG, and polylactide (PLA)–chloroform–EG, respectively.[14] The PMMA film has a pattern with shallow and deformed concavities, while the PLA film possesses a pattern with much rougher and more irregular concavities, probably because PLA is a semi-crystalline polymer and during the phase-separation of the PLA solution, the crystallization of PLA occurred and resulted in a solid–liquid demixing accompanying the liquid–liquid demixing, and, therefore, changing the final morphology of the film.

In conclusion, when keeping the film-forming parameters such as temperature and concentration unchanged, the final surface pattern is determined by the specific polymer–solvent–non-solvent combinations. In Table 3 we summarize the features of surface patterns from different polymer–solvent–non-solvent systems.

Table 3. Size and density of the surface concavities of films prepared from different polymer–solvent–non-solvent systems at 25 °C with a polymer concentration of 10 wt.-%, except for the PLA–chloroform–EG system in which the PLA concentration is 1 wt.-%.

Polymer–solvent–non-solvent system	Concavity diameter [μm]	Concavity density [features cm^{-2}]	Description
PS–cyclohexane–EG	—	—	Slowly formed, transparent, and nonporous
PS–chloroform–EG	0.5–0.6	7.3×10^6	Relatively slowly formed and semi-transparent,
PS–THF–EG	1.5–2.0	2.8×10^7	Fast formed, and well patterned
PS–THF–PF6[bmim]	0.03–0.06	4.6×10^9	Slowly formed, transparent, and well patterned
PS–THF–water	3–20	1.5×10^6	Fast formed, wide diameter distribution
PS–THF–GC	0.2–1.0	8.0×10^6	Slowly formed, and transparent
PMMA–THF–EG	2–4	9.7×10^6	Shallow, deformed concavities
PLA–chloroform–EG	1–2	4.1×10^7	Rough and irregular shaped concavities

ADVANCED FUNCTIONAL MATERIALS

2.2. Mechanism of Formation of the Patterned Film

In our method, the patterned films result from spreading a polymer solution on a non-solvent surface. The film-forming process is similar to that of separation membranes used in microfiltration, ultrafiltration, and reverse osmosis, in which a polymer solution is cast on a substrate, and immediately ,or after an appropriate evaporation period, the substrate is immersed in a non-solvent bath to induce the phase separation of the cast solution.[16] Therefore, when exploring the possible formation mechanism of the patterned film using our method, we may get some clues from the studies of the mechanism of the formation of porous membranes for filtration applications through immersion precipitation. Figure 3 compares the schematic representation of the present method (SNS) and the immersion precipitation process.

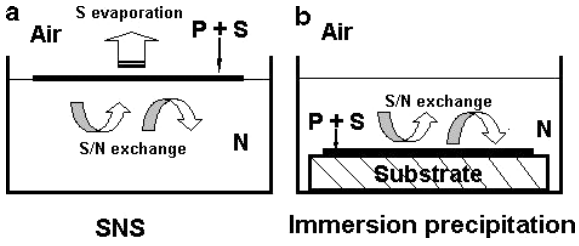

Figure 3. Schematic representation of the a) SNS and b) immersion–precipitation process: P: polymer, S: solvent, and N: non-solvent.

It has been reported that there are four main phase-separation mechanisms to produce porous membranes: thermally induced phase separation (TIPS), immersion precipitation (non-solvent-induced phase separation), air-casting of the polymer solution, and precipitation from the vapor phase.[17] Thermodynamic instability is the driving force for phase separation. Decreasing temperature, loss of solvent, or an increase in non-solvent cause a solution to become thermodynamically unstable.[18,19] In this work, the most likely mechanism of formation of the patterned films is the non-solvent-induced phase separation and/or air-casting of the polymer solution.

It is known that in the process of polymer-solution air-casting, the evaporation of the volatile solvent makes the polymer solution thermodynamically unstable and induces phase separation. In our work, volatile solvents such as THF were usually used, but the film was formed quickly by spreading the polymer solution on the non-solvent surface, usually within ten seconds, and, in such a short time, the solvent could not evaporate sufficiently to induce phase separation. In addition, we also cast the PS/THF solution on a glass substrate and allowed it to solidify in the air by solvent evaporation. We found that the polymer solution took hours to solidify and the resulting film was transparent and smooth; no pattern could be found on its surface using SEM. Practically, air-casting of polymer solution results in a dense, thin polymer film. It was reported that a highly humid atmosphere could cause phase separation of a polymer and lead to porous films in which the hexagonally packed water microdroplets formed by evaporation cooling on the solution surface served as templates for the patterned pores.[20–22] However, in the present study, the patterned films were prepared under ambient conditions with a moderate humidity (30–40 % relatively humidity). When we repeated this film-forming procedure in a dry-N_2 atmosphere, patterned films were also obtained that were not noticeably different from the films obtained under ambient conditions.

From the discussion in Section 2.1.3., we know that non-solvents play an important role in the formation of the patterned films. When a polymer solution contacts a non-solvent, there exists a strong tendency for the non-solvent to diffuse upward into the upper polymer solution, and vice versa, because the solvent and non-solvent are miscible. The mass transfer of the non-solvent and solvent across the interface causes the homogeneous solution to become thermodynamically unstable. A dense, non-porous skin is first formed at the bottom of the polymer solution because at the interface the non-solvent and solvent are in direct contact and exchange with each other very quickly. Therefore, this layer of polymer vitrifies quickly, and there is no time for pores to nucleate and grow. The solvent in the solution above the dense skin can also diffuse into the non-solvent phase through the dense skin. However, the exchange rate is significantly reduced and the change of the concentration in the polymer solution is also lowered. Thus, the phase separation of the polymer solution occurs by nucleation and growth, in which a polymer-rich phase and polymer-poor phase are formed. It has been demonstrated theoretically that the mass-transfer processes associated with most membrane-forming systems can be divided into two categories: delayed demixing and instantaneous demixing.[15,23] Almost all the membranes prepared by delayed precipitation have an open- or closed-cell structure in the sublayer. Smolders and co-workers demonstrated convincingly that nucleation and growth of a polymer-poor phase is responsible for the pore generation.[24,25] Considering the existence of the closed cells in the films, and a nonporous layer at the bottom (the side contacting the non-solvent in the film-forming procedure), we can concluded that the generation of pores in the cross-section and the concavities on the surface are the result of delayed liquid–liquid demixing by nucleation and growth of the polymer-poor phase.[15] Unlike the ball-shaped pores in the cross-section of the film, the concavities on the film surface is semispherical, as mentioned above. The difference arises from the nucleated polymer-lean phase near the polymer-solution–air interface growing upward and closer to the interface, where the growth ceases and gives many closed hemispheres. The upper layer which covers those hemispheres is formed due to the THF evaporation. It is very thin because this evaporation time is very short, and it undergoes a spinodal dewetting-induced rupture,[26,27] which gives rise to the exposed semispherical concavities on the film surface.

In conclusion, non-solvent-induced phase separation is the formation mechanism of concavity-patterned polymer films prepared via SNS.

2.3. Applications of the Patterned Surfaces

As mentioned in the Introduction, micropatterned polymer films have many applications in the fields of surface technology, microelectronic engineering, biomedicine, etc. The patterned films we fabricated through a SNS method also show some potential applications as wettability-enhancing materials, templates for micro-/nanomaterials, micro-optic components, separating membranes, etc. In the following section, we will demonstrate their applications in these aspects individually.

2.3.1. Wettability-Enhancing Materials

Wettability, which is an important property of the solid surface in practical applications, is co-governed by the chemical composition and the geometrical structure of the surfaces.[28,29] In our work, the fabricated polymer films have patterned surfaces with enhanced roughness due to the existence of many micrometer- or nanometer-scale concavities on the surface. The wettability of these films was investigated by determining their surface water contact angle.

It is reported that PS films with a smooth surface are only moderately hydrophobic with a water contact angle (CA) of about 90°,[30] while the patterned PS films prepared in this work may have an enhanced hydrophobicity as a result of the increasing surface roughness due to those micro- or nano-concavities. We tested the hydrophobicity of both sides of the patterned PS films by measuring their water CAs. As an example, the shape of a water droplet on the bottom side, which is the smooth surface contacting EG in the film-forming process, and on the top side (the patterned surface) of a PS film prepared from spreading 15 % PS/THF solution on the EG surface at 8 °C, is shown in the insets in Figs. 4a,c. The water CA on the bottom surface of the patterned film is 81.0°. However, the top, patterned surface has a CA of 120.1°, showing a significant enhancement in hydrophopicity due to the surface pattern. Moreover, it was found that the degree of hydrophobicity of the film could be adjusted by tuning the specific surface pattern. For example, Figs. 4b,c give the SEM images of two PS films with different patterned surfaces: one (Fig. 4b) has larger but fewer concavities (concavity density: 5.4×10^6 features cm^{-2}, concavity size: 2–3 μm) and the other has smaller but more concavities (concavity density: 4.4×10^7 features cm^{-2}, concavity size: 1–1.5 μm), and the shapes of the water droplets on the two films, which indicate that there is a considerable difference in their CA values, which are 98.1° and 120.1°, respectively. This difference is related to the specific surface pattern of the two films. For the film with smaller but more concavities, it provides less polymer substrate and more air gaps to support the water droplet and therefore had a more hydrophobic surface, as compared with the film with larger but fewer concavities. Furthermore, we also tested the wettability of other patterned polymer films, including PMMA and PLA, and found that all of these films showed an enhanced hydrophobicity. This indicates that the method developed in the present is a versatile technique to improve the polymer wettability.

We demonstrated here that the patterned polymer films through such a facile and versatile route have enhanced hydrophobicity. Its significance lies in that it is a very simple and cheap method to modify the surface properties of commercialized polymers, such as PS and PMMA, and more importantly, the enhancement of the polymer wettability can be achieved in a controllable way; that is, polymer films with a certain hydrophobicity can be fabricated by tuning the specific surface pattern via controlling some film-forming parameters.

2.3.2. Templates for Micro-/Nanomaterials

Nanomaterials have been the subject of intense current research because of their special physical and chemical properties that can change between the molecular and bulk limits. Consequently, there is a considerable interest in the fundamental understanding of nanomaterial properties and in their applications in electronic, optical, and mechanical devices, drug delivery, bioencapsulation, and many other fields.[31,32] Among the numerous techniques reported, template synthesis is an elegant approach[33,34] by which inorganic and organic constituents can be introduced into the void spaces of micro- or nanoporous host materials. Here we demonstrated that the polymer films with patterned surfaces prepared through such a SNS method in this work can also be used as templates.

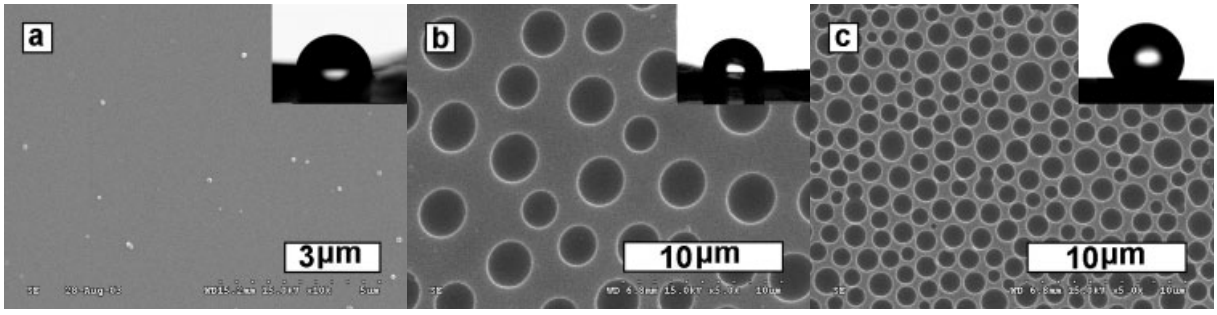

Figure 4. SEM images of the non-patterned bottom surface (a) and the patterned top surface (c)of a PS film prepared from spreading 15% PS/THF solution on an EG surface at 8 °C, and a patterned surface with larger but fewer concavities (b), prepared from spreading 8% PS/THF solution on an EG surface at 25 °C. Insets: photographs of a water droplet on the corresponding surfaces.

ADVANCED FUNCTIONAL MATERIALS

2.3.3. Convex-Patterned Polymer Films

In our previous work,[14] the PS film patterned with concavities was used as template to successfully fabricate convex-patterned polymer films. For example, PMMA/acetonitrile solution was coated on the preformed concave-patterned PS film, and acetonitrile was then evaporated in air, resulting in the PMMA/PS composite. The composite was dipped in cyclohexane at ambient temperature to dissolve the PS template, generating the convex patterned PMMA film. Figure 5a shows the convex-patterned surface of the PMMA film mould from a concave-patterned PS film with a concavity size of about 0.5–0.8 μm. Comparing with the mother template, we can see that the size and density of the convex features in the PMMA film were similar to those of the concavities in the PS templates, that is, the interior shape of the dented template concavities was faithfully copied as projected convexes. This can be explained as follows. During the coating process, the concavities in the PS films were filled by the PMMA/acetonitrile solution completely. After the evaporation of acetonitrile, a PS/PMMA composite in which concave and convex features were exactly matched and occluded was obtained. When the composite was immersed in cyclohexane, the PS template layer was gradually dissolved and released the PMMA film with the convex-patterned surface. In this method, it is most important to choose a proper solvent, which is good solvent for the convex-patterned polymer and which is a non-solvent for the concave-patterned template. We believe convex-patterned surfaces of some other polymer materials can be fabricated using suitable solvents and non-solvents for the polymers. For instance, convex-patterned PLA and poly(vinyl alcohol) (PVA) films were also fabricated using such a template-synthesis method, and Figure 5b shows a PLA film templated from a concave-patterned film with concavity size of about 2–3 μm. Similarly, the size, density, and array of the convexes on the surface completely depend on the corresponding template concavities. That is, the specific convex pattern can be tuned by choosing a proper concave-patterned template.

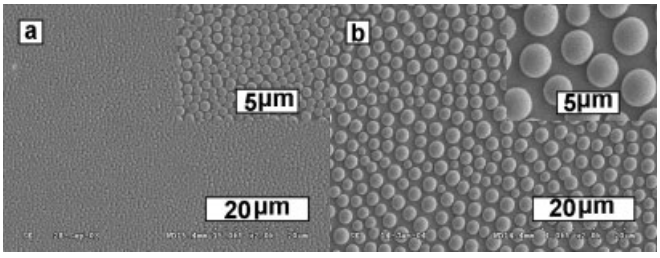

Figure 5. PMMA convex-patterned film templated from a concave-patterned film prepared from a 15 wt.-%-PS–THF–EG system at 8 °C (a) and PLA convex-patterned films templated from a concave-patterned film prepared from 10 wt.-% PS-THF-EG system at 8 °C (b).

It should be noted that the convex-patterned films also have an enhanced hydrophobicity associated with increasing surface roughness, owing to the existence of the micrometer-scale convex features on the surface.

2.3.4. Inorganic Micro-/Nanoparticles

As mentioned above, the features on the, surface of the patterned films we prepared possess a semispherical profile with a diameter of micro- or nanometer scale, and the volume of an individual concavity with a diameter of 1 μm or 100 nm is about 0.262 fL, and 2.62×10^{-4} fL, (1 fL = 1 μm^3), respectively. Therefore, these concavities can serve as micro- or nanoreactors to prepare micro-/nanoparticles. We first prepared TiO_2 microparticles by spreading a titanium precursor, tetrabutyltitanate (TBT), on the concave-patterned surface of the PS film and allowing the TBT to react with water and condense to form TiO_2. Figure 6a shows that nearly all of the concavities on the surface of the patterned PS film are occupied by a TiO_2 particle. Obviously, the size of the particles is determined by the dimensions of the featured concavities. Figure 6b indicates that the TiO_2 particles also possess a hemispherical shape, as a copy of the profile of the templating concavities.

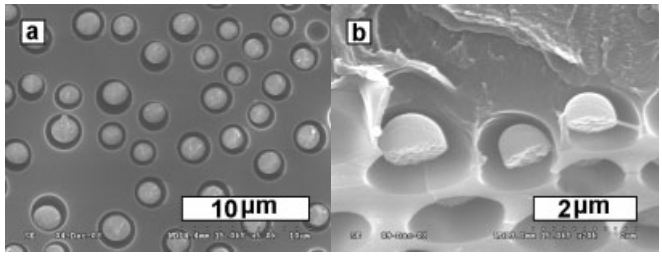

Figure 6. TiO_2 microparticles prepared in a concave-patterned PS film template: top surface (a) and cross-section (b).

In addition, we also used this surface concavities on the patterned PS film to direct the crystallization of NaCl from solution, resulting in NaCl single nanocrystals. The NaCl single nanocrystals were prepared by immersing a concave-patterned PS film in a NaCl aqueous solution and lifting it out of the solution slowly. This method is discontinuous dewetting,[35] which is straightforward and simple. As shown in Figure 7, there is a cubic NaCl crystal settled in each concavity, and the size of the crystal ranges from 100 to 150 nm, corresponding to the size of the concavity it fills. Compared with the semispherical TiO_2 particles mentioned above, it is

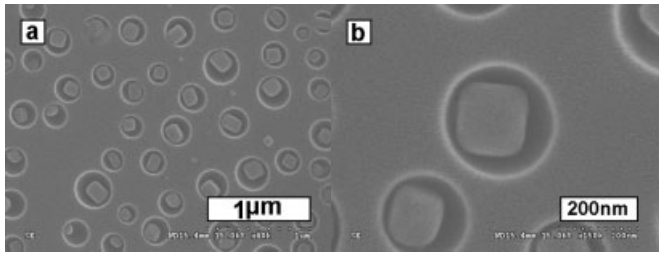

Figure 7. a,b) SEM images at different magnification of NaCl crystals in a concave-patterned PS film.

apparent that the NaCl crystals possess cubic crystal facets, rather than a copy of the mother concavities. The reason is that during the discontinuous dewetting, water in the NaCl solution filled in the concavities and evaporated, and NaCl crystallized in the concavities in the form of cubic crystals, and the templating concavity only served as a container to hold the NaCl solution while the capacity of the container, together with the solution concentration, determined the final size of the NaCl crystal.

2.3.5. Other Potential Applications

The concave-patterned and/or convex-patterned films also have other potential applications. Considering the uniform and smooth semispherical profile of the concavities, the concave-patterned films have the potential to be used as micro-spherical mirror arrays, after the inner surface of the concavities is coated with a thin layer of light-reflective materials if necessary. Furthermore, the convex-patterned films templated from the concave-patterned films can certainly be used as microlens arrays,[36–38] due to the existence of extensive, transparent, semispherical projections, and because many polymer or even inorganic materials with different abilities to refract light can be coated on the concave-patterned template. Therefore, the patterned films fabricated in this work have the potential to provide microlens arrays with different focus lengths.

In addition, based on the specific surface micropatterns, these concave- or convex-patterned polymer films also have potential applications including as scaffolds for cultivate cells, as microwells for microanalysis,[39] etc.

3. Conclusions

Thin polymer films with relatively uniform and ordered micro- or nanometer-scale concavities on their surface can be fabricated by simply spreading a polymer solution on the surface of a non-solvent for the polymer. This kind of film is probably formed through the phase separation of the polymer solution induced by the exchange between the solvent and the non-solvent. Changing the film-formation parameters, such as the polymer concentration, film-formation temperature, and polymer–solvent–non-solvent interactions, can control the specific surface pattern with the size of the concavities ranged from several micrometers to less than on hundred nanometers, and the concavity density ranged from 10^6 to 10^9 features cm^{-2}. It was confirmed that the concave-patterned polymer films possess enhanced and controllable hydrophobicity, owing to the special patterned surface. The prepared concave-patterned polymer films can be used as templates to fabricate polymer films with patterned convex features and inorganic micro-/nanopaticles that copy the shape of the concavities. The concave features in the patterned films can also be employed as a container to direct the crystallization of inorganic salts.

4. Experimental

Materials: All the polymer materials, including PS (weight-average molecular weight $M_w = 274\,370$, number-average molecular weight $M_n = 91\,230$), PMMA ($M_w = 103\,700$, $M_n = 37\,800$), PLA ($M_w = 300\,000$), PVA (degree of polymerization = 1750 ± 50), solvent, and other reagents were commercially available and used without further purification. The ionic liquid, [bmim][PF_6], was prepared using the procedures reported by Huddelstone et al. [40].

Preparation of the Concave-Patterned Films: Polymers were first dissolved in a proper solvent with agitation to prepare polymer solutions of desired concentrations. The polymer solutions were degassed by sonication. To prepare a film, about 50 μL of a solution was dropped on the surface of an appropriate non-solvent in a 35 mm diameter petri dish. After the polymer had solidified as a free-standing film, the film was then carefully removed with tweezers, washed thoroughly with ethanol, and dried in air.

Preparation of the Convex-Patterned Films: As an example, we describe the procedures to prepare PMMA convex-patterned films templated from PS concave-patterned films. PMMA/acetonitrile solution was cast on the preformed PS concave-patterned film. The acetonitrile was then evaporated in air and resulted in the PMMA/PS composite, which was then dipped in cyclohexane at ambient temperature to dissolve the PS template and generate the convex-patterned PMMA film.

Template Synthesis of TiO_2 Microparticle: Several drops of TBT were spread on a PS concave-patterned film to form a very thin liquid layer on the film surface, then the TBT-coated film was subjected to vacuum (10^{-6}MPa) at room temperature to ensure the full filling of the concavities by TBT, and subsequently immersed in 1:1 (vol./vol.) ethanol/water solution for hydrolysis for 24 h at room temperature. The hydrolyzed composite film was then wiped with a laboratory tissue soaked with ethanol to remove the attached TiO_2 surface film but leave the particles in the concavities, and finally heated under vacuum (10^{-6}MPa) overnight at 80 °C.

Template Synthesis of NaCl Nanocrystals: A concave-patterned PS film was first attached on a cover glass with the patterned surface outward using double-sided adhesive tape and then immersed in a 2 mol L^{-1} aqueous NaCl solution, and subsequently lifted out of the solution slowly, resulting in the NaCl-crystal-containing patterned film.

Characterization: All the SEM observations were made using a Hitachi S4300F field-emission scanning electron microscope. The cross-sections were obtained by fracturing samples in liquid nitrogen and all samples were sputter-coated with a 10 nm-thick layer of platinum before SEM examination. The acceleration voltage was set to 15.0 kV for all the samples, except the electron-fragile PLA films that were observed at 1.0 kV. CAs were measured on a dataphysics OCA20 contact-angle system at ambient temperature. Water droplets were dropped carefully onto the surface of samples. The average CA value was obtained by measuring at five different positions of the same sample.

Received: May 13, 2004
Final version: October 26, 2004

[1] H. Y. Erbil, A. L. Demirel, Y. Avci, O. Mert, *Science* **2003**, *299*, 1377.
[2] Y. N. Xia, G. M. Whitesides, *Angew. Chem. Int. Ed.* **1998**, *37*, 550.
[3] J. A. Rogers, K. E. Paul, *Chem. Rev.* **1999**, *99*, 1823.
[4] L. B. Goetting, T. Deng, G. M. Whitesides, *Langmuir* **1999**, *15*, 1182.
[5] W. K. Ng, L. Wu, P. M. Moran. *Appl. Phys. Lett.* **2002**, *81*, 3097.
[6] Z. Y. Zhong, B. Gates, Y. N. Xia, D. Qin, *Langmuir* **2000**, *16*, 10369.
[7] C. E. Moran, C. Radloff, N. J. Halas, *Adv. Mater.* **2003**, **15**, 804.
[8] A. Kumar, G. M. Whitesides, *Appl. Phys. Lett.* **1993**, *63*, 2002.
[9] H. Schmid, B. Michel, *Macromolecules* **2000**, *33*, 3042.
[10] J. M. Helt, C. M. Drain, J. D. Batteas, *J. Am. Chem. Soc.* **2004**, *126*, 628.

ADVANCED FUNCTIONAL MATERIALS

[11] S. A. Jenekhe, X. L. Chen, *Science* **1999**, *283*, 372.
[12] R. Ulrich, A. Du Chesne, M. Templin, U. Wiesner, *Adv. Mater.* **1999**, *11*, 141.
[13] I. W. Hamley, *Nanotechnology* **2003**, *14,* R39.
[14] Y. Wang, Z. M. Liu, B. X. Han, H. X. Gao, J. L. Zhang, K. Xun, *Chem. Commun.* **2004**, 800.
[15] P. van de Witte, P. J. Dijkstra, J. W. A. van den Berg, J. Feijen, *J. Membr. Sci.* **1996**, *117*, 1.
[16] M. Mulder, *Basic Principles of Membrane Technology,* Kluwer Academic, Dordrecht, The Netherlands **1992**.
[17] H. Matsuyama, M. Teramoto, R. Nakatani,, T. Maki, *J. Appl. Polym. Sci.* **1999**, *74*, 171.
[18] C. L. Casper, J. S. Stephens, N. G. Tassi, D. B. Chase, J. F. Rabolt, *Macromolecules* **2004**, *37*, 573.
[19] S. Megelski, J. S. Stephens, D. B. Chase, J. F. Rabolt, *Macromolecules* **2002***, 35, 8456.*
[20] G. Widawski, M. Rawiso, B. Francois. *Nature* **1994**, *369*, 387.
[21] M. Srinivasarao, D. Collings, A. Philips, S. Patel, *Science* **2001**, *292*, 79.
[22] H. Yabu, M. Tanaka, K. Ijiro, M. Shimomura, *Langmuir* **2003**, *19*, 6297.
[23] A. J. Reuvers, J. W. A. van den Berg, C. A. Smolders, *J. Membrane Sci.* **1987**, *34*, 45.
[24] A. J. Reuvers, C. A. Smolders, *J. Membrane Sci.* **1987**, *34*, 67
[25] L. Broens, D. M. Koenhen, C. A. Smolders, *Desalination* **1977**, *22*, 205.
[26] A. M. Higgins, R. A. L. Jones, *Nature* **2000**, *404*, 476.
[27] M. Boltau, S. Walheim, J. Mlynek, G. Krausch, U. Steiner, *Nature* **1998**, *391*, 877.
[28] S. H. Li, H. J. Li, X. B. Wang, Y. L. Song, Y. Q. Liu, L. Jiang, D. B. Zhu, *J. Phys. Chem. B* **2002**, *106*, 9274.
[29] G. Zhang, N. Fu, H. Zhang, J. Y. Wang, X. L. Hou, B. Yang, J. C. Shen, Y. S. Li, L. Jiang, *Langmuir* **2003**, *19*, 2434.
[30] L. Jiang, Y. Zhao, J. Zhai, *Angew. Chem. Int. Ed.* **2004**, *43*, 4338.
[31] T. N. Murakami, Y. Fukushima, Y. Hirano, Y. Tokuoka, M. Takahashi, N. Kawashima, *Colloids Surfaces B* **2003**, *29*, 171.
[32] G.M. Whitesides, J. P. Mathias, C. T. Seto. *Science* **1991,** *254*, 1312.
[33] C. R. Martin, *Science* **1994**, *266*, 1961.
[34] S. B. Lee, C. R. Martin, *Chem. Mater,* **2001**, *13*, 3236.
[35] V. R. Thalladi, G. M. Whitesides, *J. Am. Chem. Soc.* **2002**, *124*, 3520.
[36] Y. Lu, Y. D. Yin, Y. N. Xia, *Adv. Mater.* **2001**, *13*, 34.
[37] M. J. Serpe, J. S. Kim, L. A. Lyon, *Adv. Mater.* **2004**, *16*, 184.
[38] M.-H. Wu, G. M. Whitesides, *Adv. Mater.* **2002**, *14*, 1502.
[39] R. J. Jackman, D. C. Duffy, E. Ostuni, N. D. Willmore, G. M. Whitesides, *Anan. Chem.* **1998**, *70*, 2280.
[40] J. G. Huddleston, H. D. Willauer, R. P. Swatloski, A. E. Visser, R. D. Rogers, *Chem. Commun.* **1998**, 1765.

